BBA - Molecular Basis of Disease 1865 (2019) 1214–1225

Contents lists available at ScienceDirect

BBA - Molecular Basis of Disease

journal homepage: www.elsevier.com/locate/bbadis

Glaucocalyxin A-induced oxidative stress inhibits the activation of STAT3 signaling pathway and suppresses osteosarcoma progression *in vitro* and *in vivo*

Min Mao, Tao Zhang, Zhuoying Wang, Hongsheng Wang, Jing Xu, Fei Yin, Gangyang Wang, Mengxiong Sun, Zongyi Wang, Yingqi Hua*, Zhengdong Cai*

Department of Orthopaedics, Shanghai General Hospital, Shanghai Jiao Tong University School of Medicine, Shanghai, China
Shanghai Bone Tumor Institute, Shanghai, China

ARTICLE INFO

Keywords:
Glaucocalyxin A
STAT3
ROS
Oxidative stress
Osteosarcoma

ABSTRACT

Osteosarcoma (OS) is ranked as the most common primary bone malignancy in children and adolescents worldwide, and the 5-year overall survival rate of OS is not optimistic. Constitutive activation of signal transducer and activator of transcription 3 (STAT3) has been implicated in tumor cell growth, proliferation, and anti-apoptosis in OS. Therefore, the discovery of novel molecular compounds that can effectively block STAT3 activation, is essential for the treatment of OS and improving prognosis. Here, we investigate whether Glaucocalyxin A (GLA), derived from *Rabdosia japonica*, exhibit the potential anticancer effects in OS. First of all, we identify that GLA potently suppressed cell proliferation, induced G2/M phase arrest and promoted substantial apoptosis in OS. Next, we conclude that GLA could induce Reactive oxygen species (ROS)-mediated oxidative stress *via* an imbalance of GSH and GSSG. Then, we elucidate for the first time that GLA could significantly inhibit both constitutive and IL-6-inducible activation of STAT3 (Tyr705) and JAK2, the upstream regulator of STAT3. Furthermore, we elucidate that the inhibition of STAT3 is mainly induced by ROS-mediated oxidative stress. Overall, our findings demonstrate that GLA could exhibit potent anticancer effects through effectively blocking the STAT3 signaling pathway, which was induced by ROS-mediated oxidative stress in OS *in vitro* and *in vivo*.

1. Introduction

Osteosarcoma (OS), which is derived from primitive bone-forming mesenchymal cells, is ranked as the most common primary bone malignancy in children and adolescents worldwide [1]. It has been reported that the incidence of OS is 0.2–3/100,000 in children and 0.8–11/100,000 in adolescents [2]. Currently, surgical resection and neoadjuvant chemotherapy constitute the major treatment regimens for OS. However, with the advancement of surgical techniques and the application of various novel effective chemotherapy drugs, the 5-year survival rate of OS patients has been improved to 60–70% [3–5]. Unfortunately, the overall survival rate is still not optimistic, mainly because of tumor recurrence and drug resistance in recent decades. Therefore, the development of new drugs and treatment approaches is an urgent matter to improve therapeutic outcomes in OS patients.

ROS are a series of byproducts induced by oxidative stress, containing peroxides, superoxide, hydroxyl radical and singlet oxygen [6,7]. Recent accumulating evidence has demonstrated that a number of anticancer drugs, such as cisplatin, doxorubicin, and docetaxel, induce the apoptosis of cancer cells resulting from cellular ROS production [8–10]. Normally, cancer cells can tolerate oxidant stress by maintaining a balance between oxidant systems and antioxidant systems. Recent studies have demonstrated that the mechanism of ROS production by anticancer drugs is disruption of the redox balance by direct suppression of the antioxidant systems in cancer cells [11,12]. For example, glutathione (GSH) is a potent antioxidant that can

Abbreviations: GLA, Glaucocalyxin A; OS, osteosarcoma; ROS, reactive oxygen species; STAT3, signal transducer and activator of transcription 3; Jak2, Janus kinase 2; GSH, glutathione; GSSG, glutathione disulfide; NAC, *N*-acetyl-L-cysteine; GR, glutathione reductase; DMSO, dimethyl sulfoxide; BSO, buthionine sulfoximine; FBS, fetal bovine serum

* Corresponding authors at: Department of Orthopaedics, Shanghai Bone Tumor Institute, Shanghai General Hospital, Shanghai Jiao Tong University School of Medicine, Shanghai 201600, China.

E-mail addresses: yhua@shsmu.edu.cn (Y. Hua), caizhengdong@sjtu.edu.cn (Z. Cai).

https://doi.org/10.1016/j.bbadis.2019.01.016
Received 24 September 2018; Received in revised form 21 December 2018; Accepted 13 January 2019
Available online 16 January 2019
0925-4439/

eliminate cellular ROS *via* a redox reaction. Previous study has reported that upregulation of cellular GSH levels could make breast cancer cells resistant to the anticancer drug by overexpression of glutamate cysteine ligase, which is the key enzyme of GSH synthesis [13,14]. As discussed above, ROS-induced apoptosis and cell death through blocking GSH synthesis is a potential anticancer therapy for use against cancer cells.

Recent studies suggest that STAT3, a transcription factor of the STAT family, plays pivotal roles in the majority of cancers, including lung, liver, bladder, prostate, gastric cancer and OS [15–17]. Constitutive activation of STAT3 has been implicated in tumor cell growth, proliferation, and anti-apoptosis. Under normal conditions, STAT3 resides in the cytoplasm as a monomer. Upon stimulation of protein tyrosine kinases (JAKs and Src) or cytokines (IL-6 and IL-10), STAT3 is activated through the phosphorylation of the tyrosine residue (Tyr705) and subsequent dimerization. Then, activated STAT3 translocates from the cytoplasm to the nucleus and then regulates the transcriptional activation of anti-apoptotic and cell-cycle regulating gene products, such as Bcl-2, XIAP, and cyclin D1. Considering its critical role in tumor growth and progression, STAT3 has become a promising target for antitumor treatment. Currently, several reports have reported that ROS can play pivotal roles in the activity of STAT3. STAT3 itself is susceptible to oxidation in cells under oxidative stress and was shown to be modified and repressed by cysteine glutathionylation [18–20].

Natural products derived from medicinal plants have been widely used as novel anticancer drugs because of their potent efficacy and safety. Many studies have reported that many anticancer drugs isolated from natural sources, such as alterol and toosendanin, significantly suppress tumor growth and progression by inhibiting STAT3 signaling cascades [21,22]. Glaucocalyxin A (GLA), which is isolated from *Rabdosia japonica*, has been found to exhibit a wide range of pharmacological efficacies, such as inhibition of platelet activating factor-induced platelet aggregation, immunosuppressive activity, and potent anticancer properties [23–26]. The potent anticancer efficacy of GLA has been verified in multiple cancers, including liver, breast, blood and brain cancers [27–29]. These studies demonstrated that GLA exhibits antiproliferative and proapoptotic efficacies mainly mediated through inhibiting the c-jun N-terminal kinase (JNK) pathway, the serine/threonine kinase AKT pathway, or the mitochondria-mediated death pathway.

In the present study, we specifically investigated whether GLA could suppress tumor growth and induce apoptosis of OS *in vitro* and *in vivo*. As expected, we determined that the mechanism of the anticancer effect exhibited by GLA is upregulating cellular ROS production by inhibiting GSH synthesis and then abrogating both the constitutive and inducible activation of STAT3, which is essential for the growth of OS.

2. Materials and methods

2.1. Materials

Purified glaucocalyxin A (MF: $C_{20}H_{28}O_4$, MW: 332.4339, purity > 98%) was purchased from Shanghai Yuan Ye Biotechnology Co. Ltd. (Shanghai, China). It was dissolved in dimethyl sulfoxide (DMSO) as a 100 mM stock solution stored away from light in aliquots at −80 °C. The working concentrations used for different experiments were prepared by diluting the stock solution with DMSO. All the cell culture reagents were purchased from Invitrogen Life Technologies (Carlsbad, CA, USA). DMSO was obtained from Sigma-Aldrich (St. Louis, MO, USA). p-STAT3 (Tyr705) (#9145), STAT3 (#9139), Bcl-2 (#15071), PARP (#9532), cleaved PARP (#5625), caspase 3 (#9662), cleaved caspase 3 (#9661), PCNA (#2586), cyclin B1 (#4135), p-CDC2 (#4539), CDC2 (#9116), P21 (#2947), cyclin D1 (#2922), XIAP (#2042), p-JAK2 (#3771), JAK2 (#3230) and GAPDH (#5174) antibodies were purchased from Cell Signaling Technology Inc. (Danvers, MA, USA). Glutathione reductase antibody (ab124995) was purchased from Abcam (Hong Kong, China). Human IL-6, buthionine sulfoximine (BSO) and actin antibody (A1978) were purchased from Sigma-Aldrich (Sigma-Aldrich, Inc., Shanghai, China). The ROS scavenger *N*-acetyl-L-cysteine (NAC) was purchased from Beyotime (Shanghai, China), and GSH was purchased from Shenggong (Shanghai, China).

2.2. Cell culture

The cell lines 143B (human OS cells), SJSA (human OS cells), HOS (human OS cells), MG63 (human OS cells), HepG-2 (human hepatic cancer cells), A549 (human lung cancer cells), SGC7901 (human gastric cancer cells), T24 (human bladder cancer cells) and MDA-MB231 (human breast cancer cells) were purchased from the American Type Culture Collection (ATCC; Manassas, VA, USA). All cell lines were maintained in Dulbecco's modified Eagle's medium (DMEM) supplemented with 10% fetal bovine serum (FBS) plus 1% penicillin/streptomycin. Cells were maintained under standard adherent conditions at 37 °C in a humidified incubator with 5% CO_2.

2.3. Cell viability assay

Cell proliferation was determined with a CCK-8 assay (Dojindo, Tokyo, Japan). Cell suspensions (4×10^4/mL) were seeded into 96-well plates overnight and then treated with various concentrations of GLA (0, 2, 5, 10, 20 μM). GLA was dissolved in DMSO, and the concentration of DMSO was kept at < 0.05% in all wells. After 24, 48, and 72 h, 90 μL fresh medium was incubated with 10 μL CCK-8 solution in each well for 2 h at 37 °C before absorbance was read at a wavelength of 450 nm.

2.4. Colony formation assay

Cells were seeded in six-well plates at a density of 500 cells per well. In the drug treatment group, the medium was changed with fresh medium containing GLA (0.5 and 1 μM) for approximately 14 days until the cells grew into visible colonies. Colonies were fixed with 4% paraformaldehyde and stained with crystal violet for 15 min at room temperature. The colonies that consisted of 450 cells were counted.

2.5. Cell cycle analysis by flow cytometry

Cells were seeded in six-well plates at a density of 5×10^5/mL, pretreated with serum starvation for 12 h, then treated with GLA (0, 2, 4, 6 μM) for 12 h [30,31]. Then, the cells were harvested and fixed with cold 70% ethyl alcohol at 4 °C overnight. The cells were again washed with phosphate-buffered saline (PBS) and incubated with RNase A for 30 min followed by staining with 400 μL propidium iodide (PI) for 30 min at room temperature. Cell cycle analysis was performed on an Accuri C6 flow cytometer (BD Biosciences, Mountain View, CA, USA).

2.6. Apoptosis analysis by flow cytometry

The effects of GLA on cell apoptosis were analyzed by flow cytometry with Annexin V-FITC and PI. Cells were seeded in six-well plates at a density of 5×10^5/mL and treated with GLA (0, 2, 4, 6 μM) for 24 h. Then, cells were harvested, washed twice with cold PBS and resuspended in 1 × binding buffer. The cells were incubated with Annexin V-FITC and PI for 15 min in the dark at room temperature, and the samples were analyzed using an Accuri C6 flow cytometer (BD Biosciences, Mountain View, CA, USA).

2.7. Western blotting

Cells and tumor tissues were lysed with ice-cold radioimmunoprecipitation (RIPA) buffer containing protease inhibitor cocktail (Sigma-Aldrich) for 30 min. Then, soluble protein lysate concentrations were determined by using a BCA protein assay kit (Thermo Scientific, Fremont, CA, USA). Equal amounts of total protein

(20–80 μg) were resolved on 10–12% SDS-PAGE and transferred onto polyvinylidene difluoride membranes (Millipore, Billerica, MA, USA). Membranes were incubated in 5% (w/v) nonfat milk for 1 h at room temperature and incubated overnight at 4 °C on a shaker with specific primary antibodies. Membranes were washed with TBST and then incubated with secondary antibody (Sigma-Aldrich, Inc.) for 1 h at room temperature. After washing three times, the signal bands were detected by using an enhanced chemiluminescence kit (Millipore).

2.8. Establishment of STAT3 and JAK2 overexpression cell line

Human STAT3 and JAK2 were cloned into vector pcDNA3.1 to generated STAT3 and JAK2 expression plasmid. 143B cells were transiently transfected with the pcDNA3.1-STAT3 plasmid and pcDNA3.1-JAK2 plasmid through using Lipofectamine 3000 according to the manufacturer's instruction (Invitrogen, Gaithersburg, MD, USA). To produce stably transfected cells, cells were selected in the presence of puromycin (0.5 μg/mL).

2.9. Immunofluorescence assay

Cells grown on coverslips were exposed to different concentrations of GLA for 24 h, fixed with 4% paraformaldehyde, then permeabilized with 0.1% Triton X-100 in PBS. Cells were blocked with 0.5% BSA for 30 min followed by incubation with Anti-STAT3 antibody at 4 °C overnight. After washing three times, cells were probed with Alexa Fluor 488 secondary antibody for 2 h at room temperature. The nuclei were stained by 4′, 6-diamidino-2-phenylindole (DAPI). Images were acquired with a confocal microscope (Leica, Wetzlar, Germany).

2.10. RNA extraction and real-time PCR analysis

RNA samples from cells were prepared using Trizol reagent (Invitrogen, Carlsbad, CA, USA) according to the manufacturer's protocols. Total RNA (1 μg) was converted to cDNA using a Reverse Transcription Kit (TaKaRa Inc., RR036A, JAPAN). The relative expression of glutathione reductase (GR) was analyzed by RT-PCR with actin as an internal control. The primer sequences were GR: Forward 5′-CAAGCCCACAATAGAGGTCAGT-3′, Reverse 5′-AATCCATCGCTGGT TATTCCTA-3′; Actin: Forward 5-′CCGTGAAAAGATGACCCAGATC-3′, Reverse 5′-CACAGCCTGGATGGCTACGT-3′; Bcl-2: Forward 5′-ATGTG TGTGGAGAGCGTCAAC-3′, Reverse 5′-TCAGAGACAGCCAGGAGAA ATC-3′; XIAP: Forward 5′-GGCAGATTATGAAGCACGGA-3′, Reverse 5′-AATCAGTTAGCCCTCCTCCAC-3′; Cyclin D1: Forward 5′-CTGGAGC CCGTGAAAAAGA-3′, Reverse 5′-CGGATGGAGTTGTCGGTGTA-3′. Three independent experiments were carried out in triplicate.

2.11. ROS detection

The detection of intracellular ROS production was performed by using the peroxide-sensitive fluorescent probe DCFH-DA. Cells were incubated with DCFH-DA at a final concentration of 10 μM in fresh medium for 20 min at 37 °C and washed three times with fresh medium. The nuclei were stained by Hoechst 33342. ROS levels were determined by fluorescence microscopy (Leica, Wetzlar, Germany) and flow cytometry (BD Biosciences; San Jose, CA, USA).

2.12. The measurement of glutathione

The GSH/glutathione disulfide (GSSG) ratio was analyzed using a GSH and GSSG assay kit (Beyotime Inst. Biotech, S0053) following the manufacturer's instructions.

2.13. The measurement of cellular glutathione reductase

The activity of cellular GR was measured with a glutathione reductase assay kit (Beyotime Inst. Biotech, S0055). Activity was measured in mU/mL according to the manufacture's protocol. 20 μL of cellular protein was mixed with 180 μL of reaction mixture (70 μL of GR assay buffer; 10 μL of 6 mM NADPH solution; and 100 μL of GSSG solution), then add 6.6 μL DTNB solution each reaction mixture. Each experiment was carried out in triplicate on 96-well plates and absorbance was measured using a multiplate reader. The absorbance reading (A) was measured at 412 nm after mixing 0, 2, 4, 6, 8 and 10 min at 25 °C. According to the protocol, the GR activity was calculated using absorbance differences (GR activity (mU/mL) = [A_{412}/min (sample) − A_{412}/min(blank)]/0.01415.

2.14. In vivo mouse study

Four-week-old female BABL/c nude mice were assigned to the following experimental groups by stratified randomization according to body weight: a 20 mg/kg GLA group (n = 8), a 10 mg/kg GLA group (n = 8), and a vehicle (DMSO) group (n = 8). All animal procedures were performed in accordance with a protocol approved by the Animal Care and Use Committee of Shanghai General Hospital and Shanghai Jiaotong University. A total of 10^6 143B suspended cells in 20 μL PBS were injected subcutaneously in the right flank of the mice. One week after injection, each mouse in the GLA group received weight-based GLA dosage by intraperitoneal (i.p.) injection every 2 days. Mice of the vehicle group were injected with 100 μL PBS with 5% DMSO following a similar administration schedule. The tumor size was determined by Vernier calipers and calculated using the formula [length × $(width)^2$]/2. After 14 days, the mice were euthanized by cervical dislocation. Tumors were dissected and stored in liquid nitrogen or fixed in formalin for further analysis.

2.15. Hematoxylin and eosin (H&E) staining and immunohistochemistry

The hearts, lungs, kidneys, livers and spleens were fixed overnight and paraffin-embedded. Sections were subjected to H&E staining. Representative images were acquired with a Leica microscope. For immunohistochemical staining, slides were deparaffinized in xylene and rehydrate with graded alcohol and incubated in 3% H_2O_2 to block endogenous peroxidase activity. Antigen retrieval was performed by boiling in 10 mM sodium citrate (pH 6.0) for 30 min. Slides were then blocked in 10% normal goat serum for 15 min, followed by incubation with PCNA and cleaved-caspase 3 at 4 °C overnight in a moist chamber. Afterward, slides were washed three times with PBS and then incubated with the second antibody for 30 min at room temperature. Immunoreactivity was visualized using a Vectastain Elite DAB Kit (Vector Laboratories, Burlingame, CA, USA).

2.16. Statistical analysis

Data are expressed as the mean ± SD, and vertical error bars denote the SD in the figures. Student's *t*-test was used to compare two groups ($P < 0.05$ was considered statistically significant) unless otherwise indicated. To compare more than two groups, one-way ANOVA was performed ($P < 0.05$ was considered statistically significant), unless otherwise indicated. All experiments were performed at least three times except for the experiments using the animal models. No data points in our study were excluded.

3. Results

3.1. Glaucocalyxin A exhibits an inhibitory effect on proliferation and colony formation of osteosarcoma cells

The four distinct human OS cell lines (143B, SJSA, MG63, HOS) were used to investigate the antiproliferative activity of GLA (0–20 μM) by performing a Cell Counting Kit-8 (CCK-8) assay at 24, 48 and 72 h.

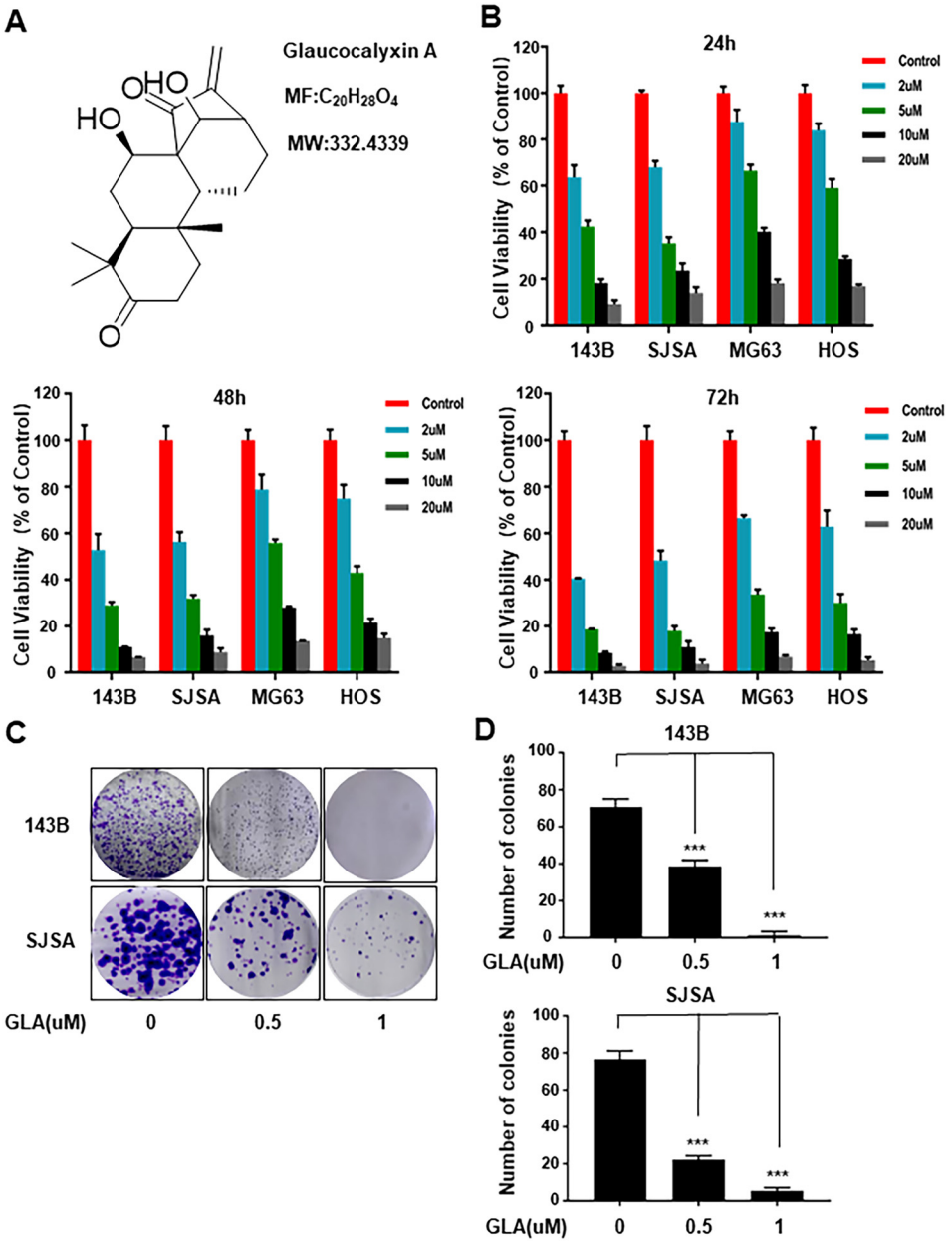

Fig. 1. GLA exhibits an inhibitory effect on proliferation and colony formation of osteosarcoma cells. (A) The chemical structural of GLA. (B) OS cell lines were exposed to the various indicated concentrations of GLA for 24, 48, or 72 h, and a CCK-8 assay was performed. (C) A colony formation assay was then performed in 143B and SJSA cells with and without GLA treatment (0.5 and 1 μM). (D) Colony numbers were counted manually. The results shown here were representative of three independent experiments. The histograms represent the mean ± SD of three independent experiments. ***P < 0.001. Significantly different compared with controls.

OS cells presented a significant dose-dependent decrease in cell viability. The IC50 values were 3.306 μM, 2.237 μM and 1.482 μM for 143B cells; 3.46 μM, 2.394 μM and 1.87 μM for SJSA cells; 8.228 μM, 6.275 μM and 3.61 μM for MG63 cells; 6.375 μM, 4.629 μM and 2.92 μM for HOS cells after 24 h, 48 h and 72 h of treatment, respectively (Fig. 1B). Next, we analyzed the clonogenicity of 143B and SJSA cell lines after GLA treatment. GLA resulted in a significant decrease in colony number (Fig. 1C and D). Collectively, these results suggested that GLA significantly inhibited the proliferation and growth of OS cells.

3.2. Glaucocalyxin A induces cell cycle G2/M arrest and substantial apoptosis in osteosarcoma cells

As cell cycle was closely related to cell growth, we detected the efficacy of GLA on the cell cycle distribution. As shown in Fig. 2A and B, flow cytometry analysis showed that GLA induced cell cycle arrest at G2/M phase, accompanied by a dose-dependent decrease in the number of G0/G1 and S phase in OS cell lines which were G0/G1 phase synchronization through pretreating with serum starvation for 12 h. In support of this conclusion, we investigated the effect of GLA on the expression of cell cycle-related proteins. Fig. 2E shows that GLA induced a significant increase in cyclin B1 and P21 and a significantly decrease in phospho-Cdc2 (p-Cdc2) with no marked change in Cdc2. These results demonstrated that GLA induced cell cycle G2/M phase arrest after 12 h of treatment by regulating cell cycle-related proteins in OS cells.

We then analyzed the efficacy of GLA in inducing apoptosis of OS cells. First, there was a marked dose-dependent increase in the percentage of apoptotic cells after 24 h of treatment according to flow cytometry (Fig. 2C and D). Additionally, western blot analysis showed that GLA induced a significant increase in cleaved caspase 3 and cleaved PARP in OS cells (Fig. 2F). Together, these results demonstrated that GLA induced substantial apoptosis in OS cells.

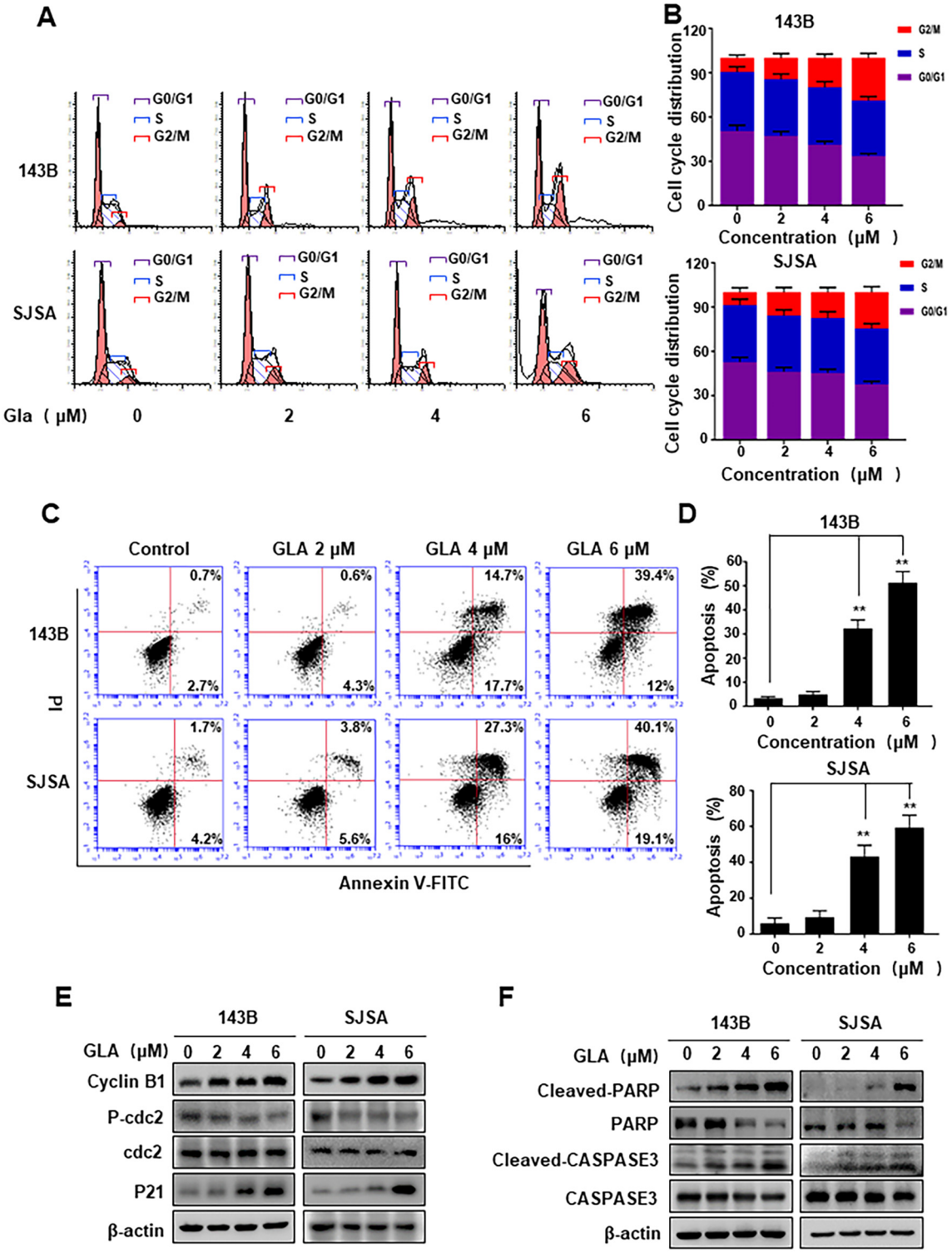

Fig. 2. GLA induces cell cycle G2/M arrest and substantial apoptosis in osteosarcoma cells (A) 143B and SJSA cells were seeded into six-well plates and pretreated with serum starvation for 12 h, then treated with various indicated concentration of GLA for 12 h. Then cells were fixed and stained with PI and analyzed by flow cytometry. (B) The percentage of cells in each cell-cycle phases is shown, which was based on three independent experiments. (C) 143B and SJSA cells were seeded into six-well plates and treated with various indicated concentration of GLA for 24 h. Then cells were stained with Annexin V and PI, and analyzed by flow cytometry. (D) The percentage of apoptotic cells among the OS cells is shown. Data are reported as the mean ± SD. (E) The protein levels of cyclin B1, p-Cdc2, Cdc2 and P21 were detected by western blot assays. (F) The protein levels of cleaved PARP, PARP, cleaved caspase3 and caspase3 were detected by western blot assays. The histograms represent the mean ± SD of three independent experiments. The results shown here are representative of three independent experiments. **P < 0.01. Significantly different compared with control.

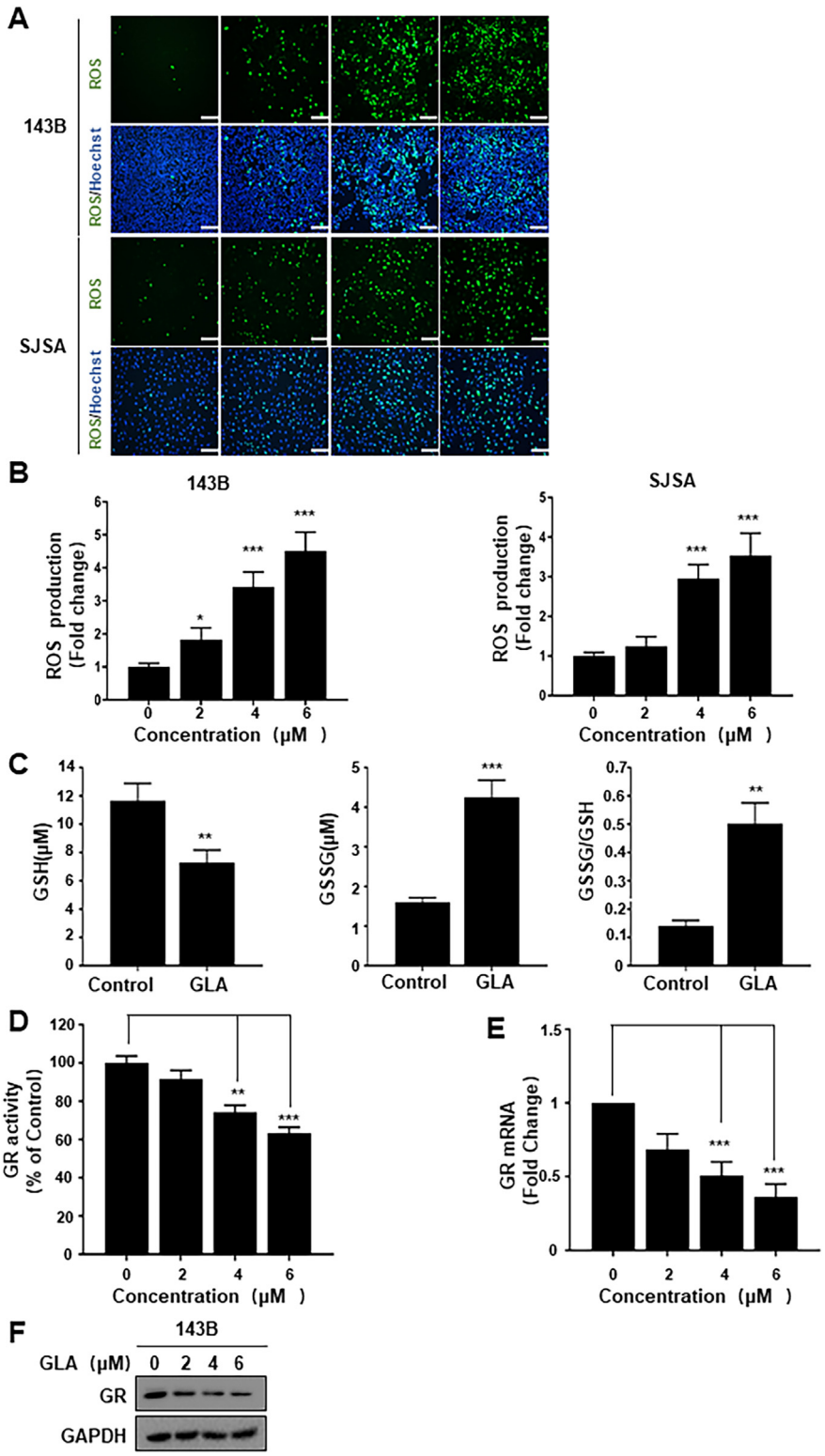

Fig. 3. GLA reduces the activity of glutathione reductase and induces reactive oxygen species production through an imbalance of GSSG/GSH. (A and B) 143B and SJSA cells were seeded into six-well plates and treated with various indicated concentrations of GLA for 12 h. Cells were loaded with 10 μM DCFH-DA for 20 min. The nuclei were stained by Hoechst 33342. The level of ROS production was detected by fluorescence microscopy (A) and flow cytometry (B). (C) 143B cells were seeded into six-well plates and treated with GLA for 12 h. The levels of GSH, GSSG and GSSG/GSH were then detected by GSH and GSSG assay kits. (D) 143B cells were seeded into six-well plates and treated with various indicated concentrations of GLA for 12 h. Then the level of GR activity was detected by a glutathione reductase assay kit. (E) 143B cells were treated with various indicated concentrations of GLA for 12 h. Total RNA was isolated and analyzed by real-time PCR analysis to detect the mRNA levels of GR. (F) The protein level of GR was detected by western blot assays. The results shown here are representative of three independent experiments. The histograms represented the mean ± SD of three independent experiments. *P < 0.05, **P < 0.01, ***P < 0.001. Significantly different compared with controls. Scale bar, 100 μm.

3.3. Glaucocalyxin A reduces the activity of glutathione reductase and induces reactive oxygen species production through an imbalance of GSSG/GSH

Next, we investigated whether oxidative stress played a pivotal role in the anticancer effect of GLA in OS cells. The level of cellular ROS was measured using a DCFH-DA probe with a fluorescence microscope and flow cytometry. We observed marked dose-dependent upregulation of ROS production after GLA exposure, demonstrating that GLA induced ROS-mediated oxidative stress in OS cells (Fig. 3A and B).

Furthermore, to explore the mechanism of ROS production after GLA treatment, we measured the concentrations of cellular GSH and GSSG. As shown in Fig. 3C and Supplementary Fig. 1A, we observed a significant decrease in GSH and an obvious increase in GSSG, suggesting that GLA can induce an imbalance of the GSSG/GSH ratio. Considering that GSSG/GSH is an important antioxidant system, we

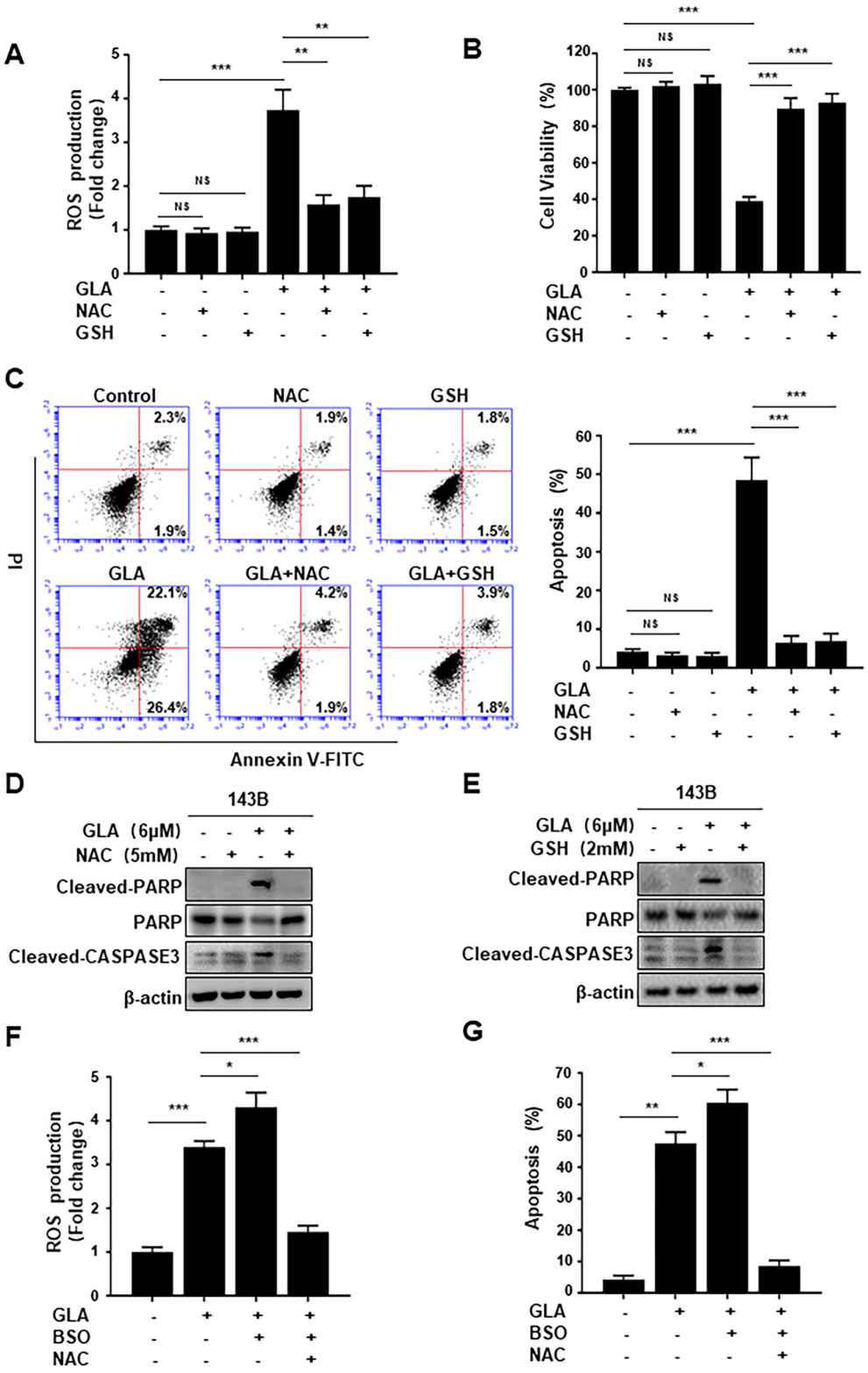

Fig. 4. Antioxidants and GSH synthesis inhibitor regulate GLA-induced inhibition of osteosarcoma cell viability and cellular apoptosis. (A) 143B cells were pretreated with NAC (5 mM) or GSH (2 mM) for 1 h and then treated with GLA (6 μM) for 12 h, The level of ROS production was detected by flow cytometry. (B) 143B cells were pretreated with NAC (5 mM) or GSH (2 mM) for 1 h and then treated with GLA (6 μM) for 24 h. Cell viability was detected by CCK8 assays. (C) 143B cells were pretreated with NAC (5 mM) or GSH (2 mM) for 1 h and then treated with GLA (6 μM) for 24 h. The apoptosis percentage of cells was detected by flow cytometry. (D and E) 143B cells were pretreated with NAC (5 mM) (D) or GSH (2 mM) (E) for 1 h and then treated with GLA (6 μM) for 24 h. The protein levels of cleaved PARP, PARP and cleaved caspase3 were detected by western blot assays. (F) 143B cells were pretreated with or without BSO (250 μM) or NAC (5 mM) for 1 h, and then treated with GLA (6 μM) for 12 h, The levels of ROS production were detected by flow cytometry.(G) 143B cells were pretreated with or without BSO (250 μM) or NAC (5 mM) for 1 h, and then treated with GLA (6 μM) for 24 h. The percentage of apoptotic cells was detected by flow cytometry. The results shown here are representative of three independent experiments. The histograms represented the mean ± SD of three independent experiments. NS: no significant different from controls, *P < 0.05, **P < 0.01, ***P < 0.001. Significantly different compared with controls.

concluded that GLA can induce upregulation of ROS production through an imbalance of GSSG/GSH. In the following experiment, we investigated how GLA influenced the balance of the GSSG/GSH system in OS cells. As GR catalyzes GSH conversion to GSSG, we measured the activity of GR after GLA treatment in OS cells. As shown in Fig. 3D and Supplementary Fig. 1B, an obvious decrease in GR activity was detected. Additionally, we examined the mRNA level and protein level of GR using real-time PCR and western blot analysis. The mRNA and protein expression levels of GR were markedly repressed after GLA treatment (Fig. 3E and F, Supplementary Fig. 1C and Fig. 1D). These results implied that GLA reduced the expression and activity of GR and then induced an imbalance of GSSG/GSH, which contributed to ROS-mediated oxidative stress. Based on these results, we concluded that GLA played an anticancer role through modulating ROS-mediated oxidative stress in OS cells.

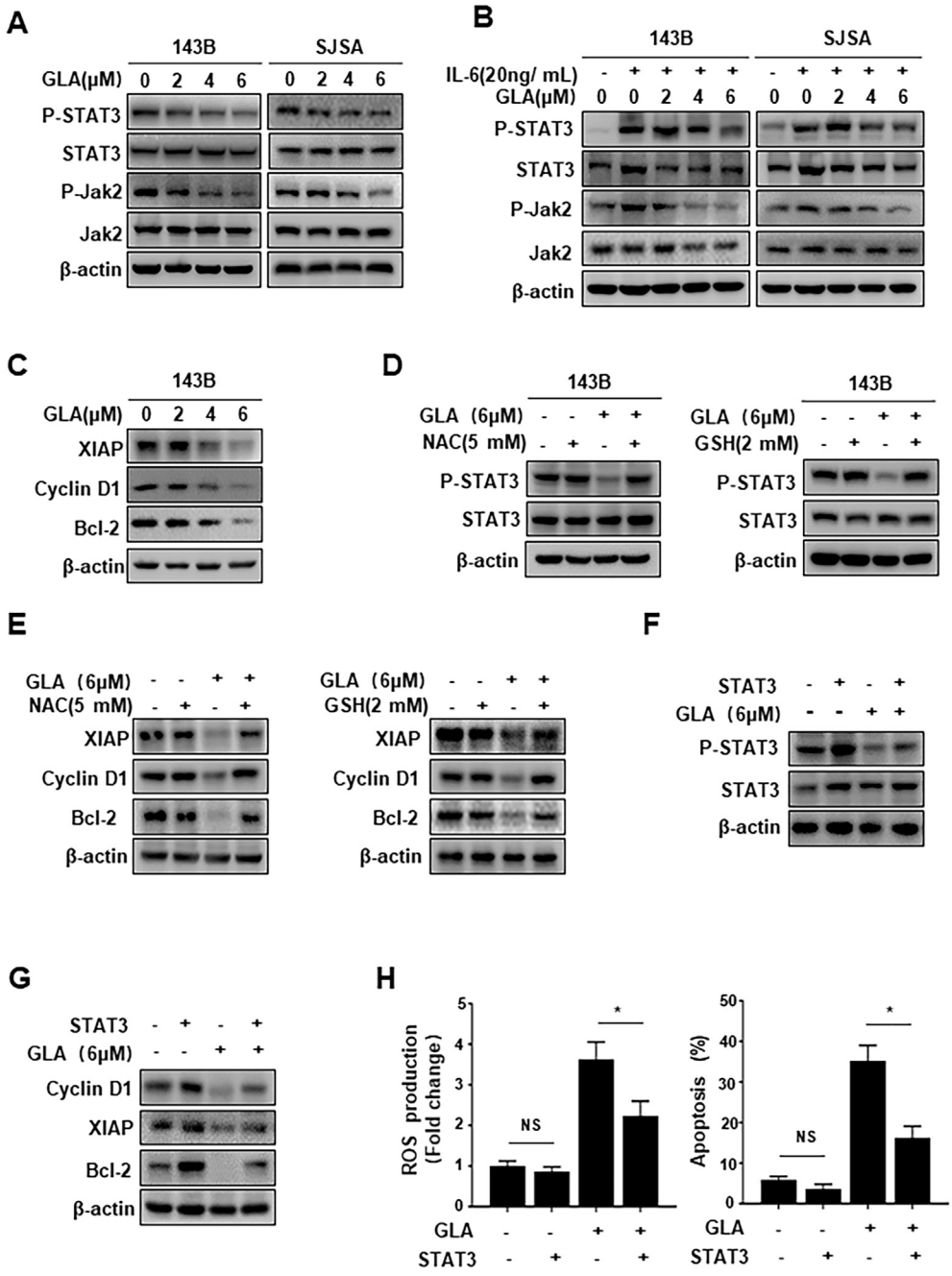

Fig. 5. GLA blocks the JAK2/STAT3 cascade in osteosarcoma cells. (A) 143B and SJSA cells were treated with various indicated concentrations of GLA for 24 h, and whole-cell extracts were prepared for western blot assays. The results shown here are representative of three independent experiments. (B) 143B and SJSA cells were treated with various indicated concentrations of GLA for 24 h, and then stimulated with IL-6 (20 ng/mL) for 30 min. (C) 143B cells were treated with various indicated concentrations of GLA for 24 h, and whole-cell extracts were prepared for western blot assays. (D and E) 143B cells were pretreated with NAC (5 mM) or GSH (2 mM) for 1 h, and then treated with GLA (6 μM) for 24 h. Whole-cell extracts were prepared for western blot assays. (F and G) 143B cells were transfected with STAT3 vector, and then treated with GLA (6 μM) for 24 h. The protein levels of p-STAT3 (Tyr705), STAT3 (F) and STAT3-targeted gene (G) were detected by western blot assays. (H) 143B cells were transfected with STAT3 vector, and then treated with GLA (6 μM) for 12 h. ROS production and apoptosis cells were detected by flow cytometry. The results shown here are representative of three independent experiments. The histograms represent the mean ± SD of three independent experiments. NS: no significant difference compared from controls, *P < 0.05, significantly different compared with controls.

3.4. Antioxidants and GSH synthesis inhibitor regulate glaucocalyxin A-induced inhibition of osteosarcoma cell viability and cellular apoptosis

To further clarify the link between oxidative stress and the anticancer effect of GLA in OS cells, we applied two ROS scavengers, NAC and GSH, to investigate the influence of antioxidants on GLA-induced inhibition of cell viability and cellular apoptosis. As shown in Fig. 4A, pretreatment with NAC and GSH apparently reduced GLA-induced ROS production. In addition, pretreatment with NAC and GSH substantially abolished the inhibition of cell viability and cellular apoptosis caused by GLA treatment (Fig. 4B and C). We also found that NAC and GSH apparently abolished the upregulation of cleaved PARP and cleaved caspase 3 caused by GLA treatment (Fig. 4D and E). Furthermore, we applied the GSH synthesis inhibitor BSO to confirm the link between GSSG/GSH and oxidative stress. Not surprisingly, we found that BSO enhanced GLA-induced ROS production and apoptosis. In addition, this combined efficacy could be reversed by NAC (Fig. 4F and G, Supplementary Fig. 1F). Collectively, these results thoroughly supported that GLA conferred an anticancer effect *via* decreased GSH and ROS-mediated oxidative stress in OS cells.

3.5. Glaucocalyxin A blocks the JAK2/STAT3 cascade in osteosarcoma cells

As a transcription factor, STAT3 plays a key role in cell proliferation and tumor growth. To elucidate the molecular mechanism of GLA-inhibited cell growth, we investigated whether the JAK2/STAT3 cascade was regulated by GLA. Western blot analysis showed that GLA significantly reduced phospho-STAT3 (Tyr705) expression, with no obvious change in STAT3 (Fig. 5A). Next, JAK2 can regulate STAT3 activation as the major upstream protein tyrosine kinase. We found that GLA highly reduced JAK2 phosphorylation in both the presence and

absence of IL-6 activation (Fig. 5A and B). As reported, STAT3 phosphorylation at Tyr705 site was critical to its biological function through promoting STAT3 cytoplasmic-to-nuclear translocation. As shown in Supplementary Fig. 2A, we found GLA can significantly inhibit IL-6-induced STAT3 nuclear accumulation, meanwhile, Supplementary Fig. 2B showed that GLA induced a significant influence on the STAT3 distribution in the cytoplasm and nucleus. In addition, STAT3 continuous activation can regulate diverse oncogenes, such as cyclin D1, Bcl-2 and XIAP, which have been reported to correlate with cell growth and cellular apoptosis. As shown in Fig. 5C and Supplementary Fig. 2C, we found that GLA significantly downregulated the protein levels and mRNA levels of cyclin D1, Bcl-2 and XIAP in dose-dependent manners. To evaluate the function of oxidative stress in JAK2/STAT3 cascade inactivation caused by GLA treatment, NAC and GSH were applied in the following experiments. As expected, pretreatment with NAC and GSH abrogated the activation of STAT3 and the expression of STAT3-regulated proteins (Fig. 5D, E and Supplementary Fig. 1E). On the basis of these results, to further confirm whether JAK2/STAT3 cascade was closely associated with GLA-induced cell death, we transfected cells with the STAT3 vector to rescue GLA-induced STAT3 inhibition. STAT3 overexpression significantly impaired GLA-induced STAT3 inhibition and STAT3-regulated gene products inhibition (Fig. 5F and G). Meanwhile, STAT3 overexpression also markedly reduced GLA-induced ROS production and attenuated GLA-induced cellular apoptosis (Fig. 5H). Then, we transfected cells with the JAK2 vector to rescue GLA-induced inactivation of STAT3 (Tyr705). JAK2 overexpression significantly increased the phosphorylation at Tyr705 residue and impaired GLA-induced inactivation of STAT3 (Tyr705) (Supplementary Fig. 2D). Meanwhile, JAK2 overexpression also obviously impaired GLA-induced STAT3-regulated gene products inhibition (Supplementary Fig. 2E). Overall, these results demonstrated that GLA initially induces ROS-mediated oxidative stress and then suppresses OS cell growth by abrogating the JAK2/STAT3 cascade, while antioxidant treatment can reverse these effects.

3.6. Glaucocalyxin A suppresses the growth of subcutaneous tumor xenografts in vivo

After elucidating the molecular mechanism of GLA-induced OS cell death *in vitro*, we examined anticancer activity of GLA on tumor growth using a xenograft mouse model. The xenograft mouse model was constructed by subcutaneous injection of 143B cells. When the subcutaneous tumors were palpable, mice were randomly divided into three groups: a 20 mg/kg GLA group, a 10 mg/kg GLA group and a vehicle group (n = 8). GLA or vehicle (DMSO) treatment was administered every 2 days for 2 weeks (Fig. 6A). The effects of GLA *in vivo* were monitored by measuring tumor volumes every 2 days. As shown in Fig. 6B, the administration of 10 mg/kg or 20 mg/kg GLA significantly inhibited OS growth. To observe the mechanism of inhibition *in vivo*, excised tumor tissues were prepared for western blot analysis and immunohistochemical analysis. The results showed that GLA reduced GR and phosphor-STAT3 (Tyr705) expression (Fig. 6C), and immunohistochemical analysis showed that GLA induced decreased expression of PCNA and increased expression of cleaved caspase 3 (Fig. 6D). Furthermore, to evaluate the potential toxicity of GLA *in vivo*, the excised major organs, including the heart, lungs, liver, spleen and kidneys, were submitted to H&E staining. The results of H&E staining revealed no obvious organ-related toxicities (Fig. 6E). Altogether, GLA significantly suppressed tumor growth of OS *in vivo*, in line with its efficacy *in vitro*.

3.7. Glaucocalyxin A inhibits the growth of other tumor cell lines

To further evaluate the anticancer effect of GLA, five other tumor cell lines (HepG-2: liver cancer; A549: lung cancer; T24: bladder cancer; SGC7901: gastric cancer; MDA-MB231: breast cancer) were used in the following experiments. Cell viabilities of other tumor cell lines were significantly inhibited by increasing concentrations of GLA (0–20 μM) (Fig. 7A). Furthermore, we asked whether the molecular mechanisms of its antitumor efficacy in OS cells were similar to those in other tumor cell lines. As expected, western blot analysis showed that GLA significantly downregulated the protein expression of GR and p-STAT3 (Tyr705) (Fig. 7B).

4. Discussion

As the 5-year overall survival rate of OS is not optimistic, the discovery of novel molecular compounds is essential for the treatment of OS to improve prognosis. In this study, we detected GLA derived from *Rabdosia japonica* and showed for the first time that this compound exhibit a significant inhibitory effect on both constitutive and IL-6-inducible activation of STAT3 (Tyr705) and JAK2, the upstream regulator of STAT3, in OS. The aim of the following experiments is to elucidate the molecular mechanism of the anticancer effects of GLA in OS cells. First, it is exciting to note that GLA leads to an imbalance of the GSSG/GSH system by reducing the activity of cellular GR. This imbalance leads to significant cellular ROS production and potent oxidative stress. Second, we show that GLA significantly suppresses STAT3 activation and downregulates the expression of various STAT3-regulated genes, thereby inhibiting proliferation and growth in OS cells and xenograft tumors. Based on these findings, we ultimately elucidate the link between ROS-mediated oxidative stress and the inhibition of JAK2/STAT3 cascades caused by GLA in OS.

It is well known that the cell cycle consists of four phases, *i.e.*, the G0/G1, S, G2/M and M phases, which are regulated by each cell cycle checkpoint. Various anticancer drugs, such as cisplatin and paclitaxel, have been recently applied to induce cancer cell death by interfering with cell cycle checkpoints, especially G2/M checkpoints [32–34]. In our study, the results fully demonstrate that GLA can induce G2/M phase arrest *via* regulating the G2/M checkpoints, including cyclin B1, CDC2 and P21 *in vitro*. In addition, given cell cycle arrest is closely associated with the apoptosis of OS cells, we further detect that GLA can induce substantial apoptosis in two distinct OS cells by flow cytometric assays. Meanwhile, we note that GLA induce apoptosis in OS cells by increasing the expression of cleaved caspase 3 and cleaved PARP. Therefore, these results demonstrate that GLA can inhibit the growth of OS cells *via* inducing G2/M phase arrest and cellular apoptosis *in vitro*.

We further observe that GLA also induce significant ROS production *in vitro*. As reported, ROS can serve dual functions in cancer cells. Hole PS *et al.* reported that low levels of ROS promote the proliferation and growth of cancer cells under normal physiological conditions [35,36]. In contrast, upregulated ROS can markedly induce apoptosis and suppress the growth of cancer cells under nonphysiological conditions, as reported by Ryter *et al.* [37]. In our study, we observe that GLA significantly inhibit cell viability and induce cellular apoptosis by upregulating ROS production, which can be reversed by two ROS scavengers, NAC and GSH. These results suggest that ROS substantially contribute to the anticancer effect of GLA in OS cells. GSSG/GSH is an important cellular anticancer system that contributes to maintaining low levels of ROS [14,38,39]. The imbalance of GSSG/GSH system reduces ROS scavenge ability. In our study, we indeed observe a significant increase in GSSG and a significant decrease in GSH after GLA treatment *in vitro*. Furthermore, BSO, GSH synthesis blocker, can enhance the effect of ROS production and apoptosis induced by GLA. These findings further demonstrate the GSSG/GSH system plays pivotal role in GLA-induced ROS production and anticancer effect. As GR can maintain the balance of the GSSG/GSH system by catalyzing the conversation of GSSG to GSH. In our study, we observe a significant inhibition of GR activity in GLA-treated OS cells, which demonstrate the inhibition of GR contribute to the imbalance of GSSG/GSH. Meanwhile, we further conclude that GR inhibition is mainly caused by the reduction of mRNA and protein levels of GR in GLA-treated OS cells.

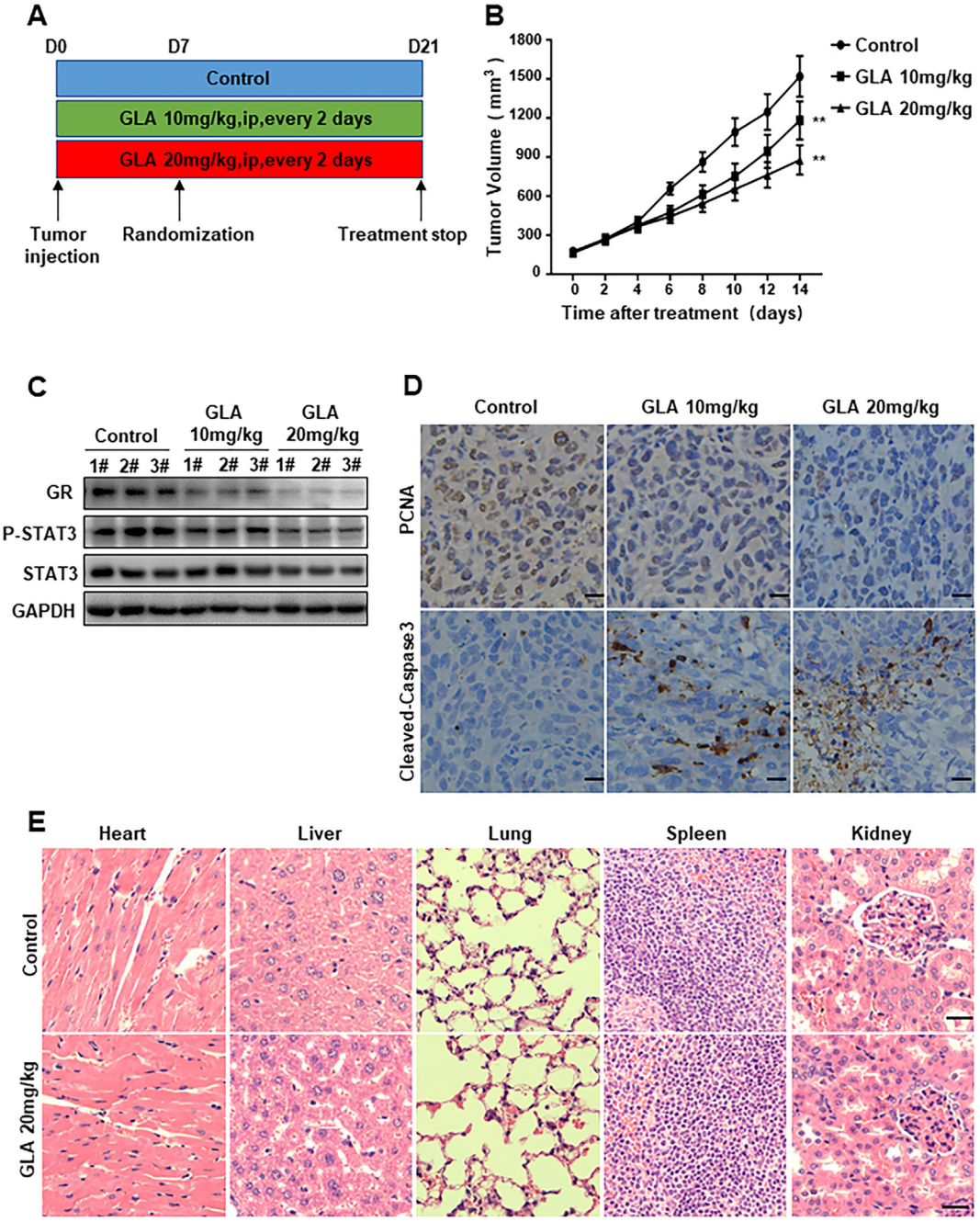

Fig. 6. GLA suppresses the growth of subcutaneous tumor xenografts *in vivo*. (A) Mice were randomly divided into three groups: a 20 mg/kg GLA group, a 10 mg/kg GLA group and a vehicle group (n = 8). GLA or vehicle (DMSO) treatment was administered every 2 days for 2 weeks. (B) Tumor volumes in mice were measured every two days. Data are shown as the mean ± SD. (C) The tumor tissues extracted were prepared for western blot assays. The protein level of p-STAT3 (Tyr705), STAT3 and GR were detected. The results shown here are representative of three independent experiments. (D) Representative pictures of PCNA and cleaved caspase3 immunostaining in tumors. Scale bar, 20 μm. (E) Major organs from the control group and the GLA-treated group were stained with H&E. Scale bar, 50 μm. **P < 0.01. Significantly different compared with controls.

Next, we for the first time demonstrate that GLA markedly suppress both constitutive and IL-6-inducible activation of STAT3 (at tyrosine 705 residue) and JAK2 which is the upstream of STAT3 in OS cells. In view of STAT3 is closely associated with the proliferation and growth of OS, we aim to elucidate the relationship between ROS-mediated oxidative stress and STAT3 inactivation. Interestingly, we observe that the inhibition of STAT3 is abolished by ROS scavengers, NAC and GSH, in GLA-treated OS cells. It has been reported that the kinase activity of JAK2 can be suppressed by ROS-mediated oxidative stress, which oxidizes the cysteine residues in the catalytic domain. Previous studies demonstrate that there are many cysteine residues located at the C-terminal region of the STAT3 Tyr705 residue, and oxidative stress can also directly oxidize these cysteines to suppress the phosphorylation of STAT3 [40,41]. In our study, we also note that GLA-induced ROS production and cellular apoptosis can be partially reversed by STAT3 overexpression. Thus, these findings demonstrate that GLA can abrogate STAT3 activation *via* ROS-mediated oxidative stress and then inhibit the growth of OS cells *in vitro*.

Finally, we investigate the anticancer effect of GLA in a xenograft mouse model. Our study for the first time demonstrate that GLA can significantly inhibit the growth of OS by abrogating GR expression and STAT3 activation *in vivo*, which correlates well with its observed *in vitro*

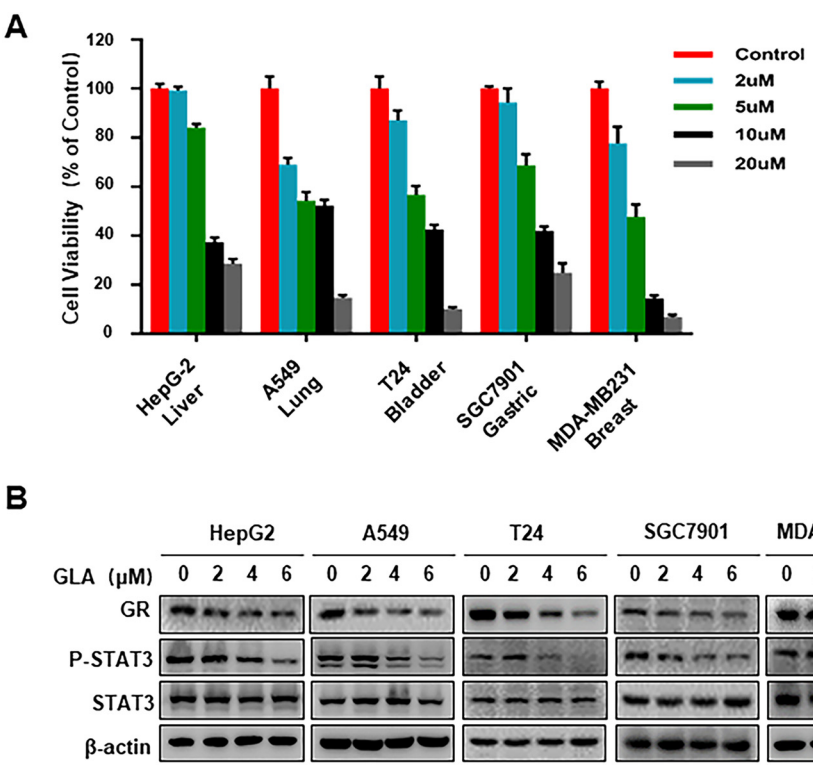

Fig. 7. GLA inhibits the growth of other tumor cell lines. (A) Various cancer cells were treated with the indicated concentrations of GLA for 24 h, and a CCK-8 assay was performed. The histograms represent the mean ± SD of three independent experiments. (B) Tumor cells were treated with various indicated concentration of GLA for 24 h. Samples were immunoblotted using the indicated antibodies. The results shown here are representative of three independent experiments.

effect. In addition, no obvious major organ toxicity was observed in the GLA-treated OS mouse model.

In conclusion, our findings for the first time suggest that GLA can significantly suppress the growth of OS through blocking STAT3 signaling pathway which is mainly regulated by ROS-mediated oxidative stress. Moreover, no other studies have reported a therapeutic effect of GLA using an OS mouse model. Our findings clearly demonstrate that GLA can be developed as a novel and potential anticancer drug for the treatment of OS.

Supplementary data to this article can be found online at https://doi.org/10.1016/j.bbadis.2019.01.016.

Funding

This project was supported by the NSFC (81502604, 81501584, and 81702973), the Shanghai Science and Technology Committee (14140904000), the Doctoral Innovation Fund of Shanghai Jiao Tong University School of Medicine (No. BXJ201732), the Shanghai Municipal Commission of Health and Family Planning Foundation (No. 20164Y0270), and a Research Grant from the Shanghai Hospital Development Center (SHDC12013107).

Transparency document

The Transparency document associated with this article can be found, in online version.

Acknowledgements

The authors thank the Institute of Central Laboratory of Shanghai General Hospital for providing parts of the experimental apparatus. We also thank Mr. Lang Tao and Mr. Tang Jinhua (Shanghai General Hospital, Shanghai Jiao Tong University School of Medicine) for their assistance.

Conflict of interest

The authors declare no conflict of interest.

References

[1] G. Ottaviani, N. Jaffe, The epidemiology of osteosarcoma, Cancer Treat. Res. 152 (2009) 3–13.
[2] L. Mirabello, R.J. Troisi, S.A. Savage, Osteosarcoma incidence and survival rates from 1973 to 2004: data from the Surveillance, Epidemiology, and End Results Program, Cancer 115 (2009) 1531–1543.
[3] L.A. Doyle, Sarcoma classification: an update based on the 2013 World Health Organization Classification of Tumors of Soft Tissue and Bone, Cancer 120 (2014) 1763–1774.
[4] H. Wang, W. Sun, M. Sun, Z. Fu, C. Zhou, C. Wang, D. Zuo, Z. Zhou, G. Wang, T. Zhang, J. Xu, J. Chen, Z. Wang, F. Yin, Z. Duan, F.J. Hornicek, Z. Cai, Y. Hua, HER4 promotes cell survival and chemoresistance in osteosarcoma via interaction with NDRG1, Biochim. Biophys. Acta 1864 (2018) 1839–1849.
[5] K.R. Duchman, Y. Gao, B.J. Miller, Prognostic factors for survival in patients with high-grade osteosarcoma using the Surveillance, Epidemiology, and End Results (SEER) Program database, Cancer Epidemiol. 39 (2015) 593–599.
[6] G.S. Shadel, T.L. Horvath, Mitochondrial ROS signaling in organismal homeostasis, Cell 163 (2015) 560–569.
[7] E. Gammella, S. Recalcati, G. Cairo, Dual role of ROS as signal and stress agents: iron tips the balance in favor of toxic effects, Oxidative Med. Cell. Longev. 2016 (2016) 8629024.
[8] S. Gao, T. Chen, M.Y. Choi, Y. Liang, J. Xue, Y.S. Wong, Cyanidin reverses cisplatin-induced apoptosis in HK-2 proximal tubular cells through inhibition of ROS-mediated DNA damage and modulation of the ERK and AKT pathways, Cancer Lett. 333 (2013) 36–46.
[9] H. Wang, Z. Gao, X. Liu, P. Agarwal, S. Zhao, D.W. Conroy, G. Ji, J. Yu, C.P. Jaroniec, Z. Liu, X. Lu, X. Li, X. He, Targeted production of reactive oxygen species in mitochondria to overcome cancer drug resistance, Nat. Commun. 9 (2018) 562.
[10] J. Shen, X. Sheng, Z. Chang, Q. Wu, S. Wang, Z. Xuan, D. Li, Y. Wu, Y. Shang, X. Kong, L. Yu, L. Li, K. Ruan, H. Hu, Y. Huang, L. Hui, D. Xie, F. Wang, R. Hu, Iron metabolism regulates p53 signaling through direct heme-p53 interaction and modulation of p53 localization, stability, and function, Cell Rep. 7 (2014) 180–193.
[11] J. Zhang, K.S. Ahn, C. Kim, M.K. Shanmugam, K.S. Siveen, F. Arfuso, R.P. Samym, A. Deivasigamanim, L.H. Lim, L. Wang, B.C. Goh, A.P. Kumar, K.M. Hui, G. Sethi, Nimbolide-induced oxidative stress abrogates STAT3 signaling cascade and inhibits tumor growth in transgenic adenocarcinoma of mouse prostate model, Antioxid. Redox Signal. 24 (2016) 575–589.
[12] X.J. Wang, Y. Li, L. Luo, H. Wang, Z. Chi, A. Xin, X. Li, J. Wu, X. Tang, Oxaliplatin activates the Keap1/Nrf2 antioxidant system conferring protection against the cytotoxicity of anticancer drugs, Free Radic. Biol. Med. 70 (2014) 68–77.

[13] K.K. Andringa, M.C. Coleman, N. Aykin-Burns, M.J. Hitchler, S.A. Walsh, F.E. Domann, D.R. Spitz, Inhibition of glutamate cysteine ligase activity sensitizes human breast cancer cells to the toxicity of 2-deoxy-D-glucose, Cancer Res. 66 (2006) 1605–1610.
[14] R.J. Mailloux, D. Craig Ayre, S.L. Christian, Induction of mitochondrial reactive oxygen species production by GSH mediated S-glutathionylation of 2-oxoglutarate dehydrogenase, Redox Biol. 8 (2016) 285–297.
[15] T. Zhang, S. Li, J. Li, F. Yin, Y. Hua, Z. Wang, B. Lin, H. Wang, D. Zou, Z. Zhou, J. Xu, C. Yi, Z. Cai, Natural product pectolinarigenin inhibits osteosarcoma growth and metastasis via SHP-1-mediated STAT3 signaling inhibition, Cell Death Dis. 7 (2016) e2421.
[16] W.J. Wang, C.F. Li, Y.Y. Chu, Y.H. Wang, T.C. Hour, C.J. Yen, W.C. Chang, J.M. Wang, Inhibition of the EGFR/STAT3/CEBPD axis reverses cisplatin cross-resistance with paclitaxel in the urothelial carcinoma of the urinary bladder, Clin. Cancer Res. 23 (2017) 503–513.
[17] N. Don-Doncow, F. Marginean, I. Coleman, P.S. Nelson, R. Ehrnstrom, A. Krzyzanowska, C. Morrissey, R. Hellsten, A. Bjartell, Expression of STAT3 in prostate cancer metastases, Eur. Urol. 71 (2017) 313–316.
[18] L. Li, P.E. Shaw, A STAT3 dimer formed by inter-chain disulphide bridging during oxidative stress, Biochem. Biophys. Res. Commun. 322 (2004) 1005–1011.
[19] Y. Xie, S. Kole, P. Precht, M.J. Pazin, M. Bernier, S-glutathionylation impairs signal transducer and activator of transcription 3 activation and signaling, Endocrinology 150 (2009) 1122–1131.
[20] X. Zhang, S. Zhang, Q. Sun, W. Jiao, Y. Yan, X. Zhang, Compound K induces endoplasmic reticulum stress and apoptosis in human liver cancer cells by regulating STAT3, Molecules 23 (2018).
[21] T. Zhang, J. Li, F. Yin, B. Lin, Z. Wang, J. Xu, H. Wang, D. Zuo, G. Wang, Y. Hua, Z. Cai, Toosendanin demonstrates promising antitumor efficacy in osteosarcoma by targeting STAT3, Oncogene 36 (2017) 6627–6639.
[22] D. Zuo, Z. Zhou, H. Wang, T. Zhang, J. Zang, F. Yin, W. Sun, J. Chen, L. Duan, J. Xu, Z. Wang, C. Wang, B. Lin, Z. Fu, Y. Liao, S. Li, M. Sun, Y. Hua, L. Zheng, Z. Cai, Alternol, a natural compound, exerts an anti-tumour effect on osteosarcoma by modulating of STAT3 and ROS/MAPK signalling pathways, J. Cell. Mol. Med. 21 (2017) 208–221.
[23] M. Li, X.G. Jiang, Z.L. Gu, Z.B. Zhang, Glaucocalyxin A activates FasL and induces apoptosis through activation of the JNK pathway in human breast cancer cells, Asian Pac. J. Cancer Prev. 14 (2013) 5805–5810.
[24] M.S. Ur Rahman, L. Zhang, L. Wu, Y. Xie, C. Li, J. Cao, Sensitization of gastric cancer cells to alkylating agents by glaucocalyxin B via cell cycle arrest and enhanced cell death, Drug Des. Devel. Ther. 11 (2017) 2431–2441.
[25] Z. Xiang, X. Wu, X. Liu, Y. Jin, Glaucocalyxin A: a review, Nat. Prod. Res. 28 (2014) 2221–2236.
[26] J. Zhu, Y. Sun, Y. Lu, X. Jiang, B. Ma, L. Yu, J. Zhang, X. Dong, Q. Zhang, Glaucocalyxin A exerts anticancer effect on osteosarcoma by inhibiting GLI1 nuclear translocation via regulating PI3K/Akt pathway, Cell Death Dis. 9 (2018) 708.
[27] W. Lin, J. Xie, N. Xu, L. Huang, A. Xu, H. Li, C. Li, Y. Gao, M. Watanabe, C. Liu, P. Huang, Glaucocalyxin A induces G2/M cell cycle arrest and apoptosis through the PI3K/Akt pathway in human bladder cancer cells, Int. J. Biol. Sci. 14 (2018) 418–426.
[28] L. Tang, X. Jin, X. Hu, X. Hu, Z. Liu, L. Yu, Glaucocalyxin A inhibits the growth of liver cancer Focus and SMMC-7721 cells, Oncol. Lett. 11 (2016) 1173–1178.
[29] Y. Liu, S. Lu, L. Zhao, X. Dong, Z. Zhu, Y. Jin, H. Chen, F. Lu, Z. Hong, Y. Chai, Effects of glaucocalyxin A on human liver cancer cells as revealed by GC/MS- and LC/MS-based metabolic profiling, Anal. Bioanal. Chem. 410 (2018) 3325–3335.
[30] N. Saleh-Gohari, T. Helleday, Conservative homologous recombination preferentially repairs DNA double-strand breaks in the S phase of the cell cycle in human cells, Nucleic Acids Res. 32 (2004) 3683–3688.
[31] T. Bertero, C. Gastaldi, I. Bourget-Ponzio, B. Mari, G. Meneguzzi, P. Barbry, G. Ponzio, R. Rezzonico, CDC25A targeting by miR-483-3p decreases CCND-CDK4/6 assembly and contributes to cell cycle arrest, Cell Death Differ. 20 (2013) 800–811.
[32] T. Shingu, V.C. Chumbalkar, H.S. Gwak, K. Fujiwara, S. Kondo, N.P. Farrell, O. Bogler, The polynuclear platinum BBR3610 induces G2/M arrest and autophagy early and apoptosis late in glioma cells, Neuro-Oncology 12 (2010) 1269–1277.
[33] M. Vallon, C. Seidl, B. Blechert, Z. Li, K.P. Gilbertz, A. Baumgart, M. Aichler, A. Feuchtinger, F.C. Gaertner, F. Bruchertseifer, A. Morgenstern, A.K. Walch, R. Senekowitsch-Schmidtke, M. Essler, Enhanced efficacy of combined 213Bi-DTPA-F3 and paclitaxel therapy of peritoneal carcinomatosis is mediated by enhanced induction of apoptosis and G2/M phase arrest, Eur. J. Nucl. Med. Mol. Imaging 39 (2012) 1886–1897.
[34] H. Wang, T. Zhang, W. Sun, Z. Wang, D. Zuo, Z. Zhou, S. Li, J. Xu, F. Yin, Y. Hua, Z. Cai, Erianin induces G2/M-phase arrest, apoptosis, and autophagy via the ROS/JNK signaling pathway in human osteosarcoma cells in vitro and in vivo, Cell Death Dis. 7 (2016) e2247.
[35] P.S. Hole, J. Zabkiewicz, C. Munje, Z. Newton, L. Pearn, P. White, N. Marquez, R.K. Hills, A.K. Burnett, A. Tonks, R.L. Darley, Overproduction of NOX-derived ROS in AML promotes proliferation and is associated with defective oxidative stress signaling, Blood 122 (2013) 3322–3330.
[36] J.Dong Lu, L. Wang, Q. Xia, D. Zhang, H. Kim, T. Yin, S. Fan, Q. Shen, Activation of STAT3 and Bcl-2 and reduction of reactive oxygen species (ROS) promote radioresistance in breast cancer and overcome of radioresistance with niclosamide, Oncogene 37 (2018) 5292–5304.
[37] S.W. Ryter, H.P. Kim, A. Hoetzel, J.W. Park, K. Nakahira, X. Wang, A.M. Choi, Mechanisms of cell death in oxidative stress, Antioxid. Redox Signal. 9 (2007) 49–89.
[38] S. Golbidi, A. Botta, S. Gottfred, A. Nusrat, I. Laher, S. Ghosh, Glutathione administration reduces mitochondrial damage and shifts cell death from necrosis to apoptosis in ageing diabetic mice hearts during exercise, Br. J. Pharmacol. 171 (2014) 5345–5360.
[39] D. Giustarini, I. Dalle-Donne, R. Colombo, A. Milzani, R. Rossi, An improved HPLC measurement for GSH and GSSG in human blood, Free Radic. Biol. Med. 35 (2003) 1365–1372.
[40] C. Kim, S.G. Lee, W.M. Yang, F. Arfuso, J.Y. Um, A.P. Kumar, J. Bian, G. Sethi, K.S. Ahn, Formononetin-induced oxidative stress abrogates the activation of STAT3/5 signaling axis and suppresses the tumor growth in multiple myeloma preclinical model, Cancer Lett. 431 (2018) 123–141.
[41] Z. Zhang, Q. Duan, H. Zhao, T. Liu, H. Wu, Q. Shen, C. Wang, T. Yin, Gemcitabine treatment promotes pancreatic cancer stemness through the Nox/ROS/NF-kappaB/STAT3 signaling cascade, Cancer Lett. 382 (2016) 53–63.